The International Journal of Advanced Manufacturing Technology (2019) 102:3767–3779
https://doi.org/10.1007/s00170-019-03377-y

ORIGINAL ARTICLE

Research on roll forming process based on five-boundary condition forming angle distribution function

Chun-Jian Su[1] · Long-Yun Yang[1] · Shu-Mei Lou[1] · Qing Wang[2] · Rui Wang[1]

Received: 12 April 2018 / Accepted: 21 January 2019 / Published online: 27 February 2019
© Springer-Verlag London Ltd., part of Springer Nature 2019

Abstract

Process parameters crucially influence product quality in complex roll-forming process. Improper setting of process parameters can cause springback and peak longitudinal strain, resulting in product defects. In the present study, the main process parameters considered are forming angle and sheet thickness. The forming angle for each pass of forming is allocated reasonably by applying a five-boundary condition, which forms an angle distribution function, to further study the effects of sheet thickness and material properties on the peak longitudinal strain and springback. Moreover, transverse strain in the bending zone was studied based on the microstructure of the sheet used herein. The results of finite element simulation and experiments demonstrate that the peak longitudinal strain increases with increase in the forming angle. The peak longitudinal strain decreases with the sheet thickness increases, while the transverse strain increases with the sheet thickness increases. The springback decreases with the increase of sheet thickness under the condition of a certain roll radius. The continuous forming springback angle between the first and the ninth forming passes was only 0.5° in the paper. The peak longitudinal strain and springback are closely related to material properties.

Keywords Roll forming · Process parameters · Peak longitudinal strain · Springback

1 Introduction

Roll forming is used to obtain specific cross-sectional shapes by means of transverse sheet bending by using multi-pass forming rollers [1, 2]. It is a continuous, efficient, and high-quality metal forming process, and it is shown schematically in Fig. 1. A sheet is formed using a certain sequence of different shapes of the upper forming roll and the lower forming roll until it is bent into the desired shape [3]. Roll forming conserves material, affords satisfactory surface precision and forming quality, has high production efficiency, and it is not limited in terms of the cross-sectional sizes and shapes that can be created. The method is now widely used in varied domains such as construction, automobile manufacturing, and aerospace [4, 5].

The increment in forming angle between passes, yield limit and sheet thickness are important process parameters in roll forming. These parameters significantly influence formed products. Bidabadi et al. [6, 7] studied the longitudinal bowing of symmetric U-channel sections in cold roll forming by means of experiments and finite element simulation. The results demonstrated that the most important forming parameters are forming angle increment between forming passes, flange width, and sheet thickness. Liu et al. [8] developed a new mathematical model to analyse the distribution of forming angle and the development of longitudinal strain in the roll-forming deformation process. The results indicate that longitudinal strain is related to roll geometry and transverse cross-section of the sheet. Lindgren's [9] research demonstrated that the yield strength of the material affects the profile of the finished product, and with increasing yield strength of the sheet, the longitudinal peak membrane strain decreases, which is contrary to the results of the present study. Yan et al. [10] found that the Hill 48 yield criterion solved using the stress

✉ Rui Wang
wangrui_ysu@foxmail.com

Long-Yun Yang
yanglongyun2016@163.com

[1] College of Mechanical and Electronic Engineering, Shandong University of Science and Technology, Qingdao 266590, People's Republic of China

[2] School of material science and engineering, Shandong University of Science and Technology, Qingdao 266590, People's Republic of China

method can well reflect the material deformation behaviour under the plane strain condition. Liu et al. [11] applied the linear regression method to evaluate the effect on local thickness reduction. The results indicated that the loading pattern and the roll diameter have the greatest influences on local thickness reduction and transverse strain in the bending zone.

The unreasonable distribution of forming angle increment and the material properties can induce the peak longitudinal strain, which leads to product defects. Therefore, it is very important to reduce the peak longitudinal strain in roll forming [12]. Abeyrathna et al. [13, 14] showed that the process and shape parameters of the parts significantly affect the peak longitudinal edge strain, which causes product defects. Their results showed that the peak longitudinal edge strain and springback increase as the yield strength increases. In-line shape compensation methods have been used to study the effect of material properties on common shape defects during roll forming. Han et al. [15] used the B3-spline finite strip method and found that the peak longitudinal strain increases with decreasing sheet thickness and increases with increasing material yield strength. Paralikas et al. [16] used advanced high-strength steel (AHSS) (DP series and TRIP series) to analyse the effects of sheet thickness on the longitudinal and transverse strain distributions and springback of the final shape product. Zeng et al. [17] optimised the forming process by using springback angle as the objective function and edge membrane longitudinal strain as the constraining condition. The results show that the precision of forming was improved and edge wave defects in products were eliminated. Abeyrathna et al. [18] showed that the peak longitudinal strain near the point of roll contact is large, and longitudinal strains in roll forming are often associated with shape defects such as bow, warping, and end flare. Rezaei et al. [19] verified that longitudinal edge strains lead to increased web warping. Liu and Huang [20] performed a three-roll-push-bending study and found that the springback angle increases as the bending radius and wall thickness increase.

Before conducting this study, based on actual production experience and theoretical analysis, the authors successfully proposed the forming angle distribution function based on a five-boundary condition and constructed the projection track of the edge of the profile section in the horizontal plane that follows a cubic curve. It was proved that the forming angle distribution was the best when the forming angle of the first third of the forming passes was $30\,\% \times \theta_0 \le \theta_{N/3} \le 35\,\% \times \theta_0$. The forming angle distribution was studied based on the five-boundary condition forming angle distribution function $\theta_{N/3} = 33\,\% \times \theta_0$. Then, the effects of material properties and sheet thickness on the peak longitudinal strain distribution and springback angle during roll forming were studied. Simultaneously, the transverse strain in the bending zone was studied based on the metal microstructure.

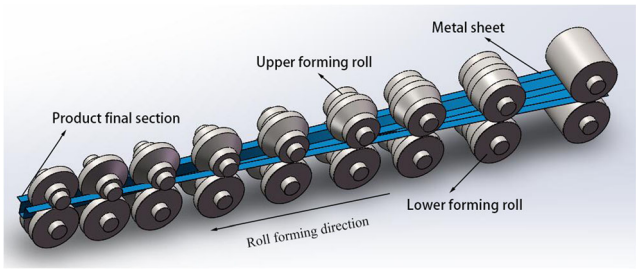

Fig. 1 Roll-forming process

2 Finite element simulation

2.1 Distribution of forming angle

In a study on forming angle distribution in roll forming, Ona et al. [21] state that the projection track of the edge of the profile section in the horizontal plane that follows a cubic curve, that is

$$y = Ax^3 + Bx^2 + Cx + D \tag{1}$$

as shown in Fig. 2, distribution of the forming angle in roll forming is optimal when the projection of the lateral end of the sheet follows the curve. Equation (1) was derived by Ona et al. [21], a Japanese scholar, who sorted out the design data, forming process drawings and longitudinal bowing forming experiment

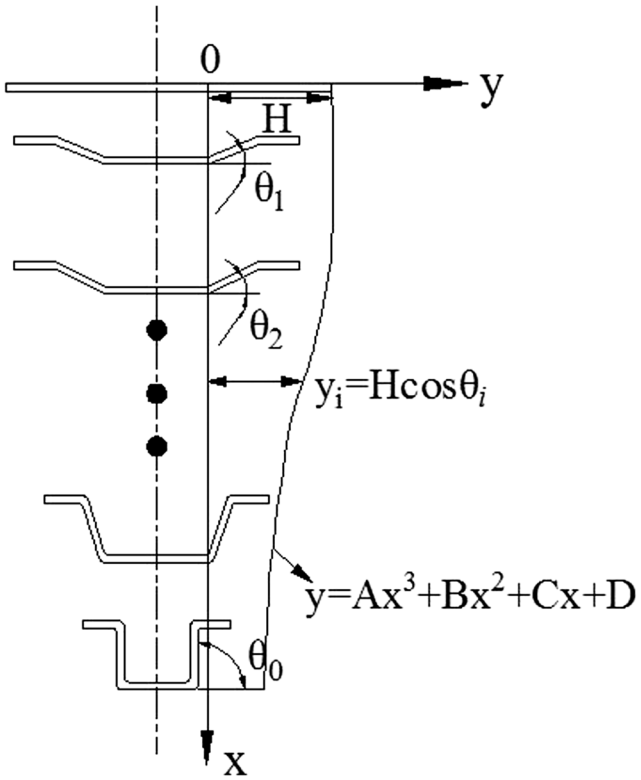

Fig. 2 Projection track of the edge of a hat-shaped steel section in the horizontal plane

Table 1 Forming angle distribution of four-boundary condition

	Forming pass number								
i	1	2	3	4	5	6	7	8	9
θ_i	15.0	29.1	42.2	54.3	65.4	75.0	82.7	88.0	90.0
$\Delta\theta_i$	15.0	14.1	13.1	12.1	11.1	9.6	7.7	5.3	2.0

of roll forming of various companies. In roll forming, it is considered that the bending of the sheet metal at the beginning portion (front portion) and the end part (final portion) is formed to a lesser extent, but the middle part (middle portion) is formed to a greater extent, and Eq. (1) can be obtained by functionalizing this empirical rule. It assumes that N is the total number of forming passes, θ_i is forming angle in the ith pass, θ_0 is final forming angle, H is length of the stand side, the coordinates X of Fig. 2 is the longitudinal length of the sheet, the unit is mm, and distance between two roll stations is equal.

Based on an analysis of the roll-forming process shown in Fig. 2, the four-boundary condition of Eq. (1) can be expressed as Eq. (2):

$$\begin{cases} \dfrac{dy}{dx} = 0, (\mathrm{x} = 0) \\ \dfrac{dy}{dx} = 0, (x = N) \\ y = H, (\mathrm{x} = 0) \\ y = H\cos\theta_0, (\mathrm{x} = N) \end{cases} \tag{2}$$

When $x = i$, $y_i = H\cos\theta_i$; thus, the forming angle in the ith pass θ_i in roll forming is

$$\cos\theta_i = 1 + (1-\cos\theta_0)\left[2\left(\frac{i}{N}\right)^3 - 3\left(\frac{i}{N}\right)^2\right] \tag{3}$$

Substituting $i = 1, 2, \ldots, N$ into Eq. (3), we obtain the forming angle of each pass.

In this study, we continue to use the relationship curve between shape factors and forming passes given in the Roll Forming Handbook, and the number of roll forming passes was calculated as nine [22]. Therefore, according to the four-boundary condition, the forming angle distribution function to calculate the distribution of each pass angle is given in Table 1.

Table 2 Forming angle distribution for each pass of 33 % $\times\theta_0$

$\theta_{N/3}$		Forming pass number								
33 % $\times\theta_N$	i	1	2	3	4	5	6	7	8	9
	θ_i	7.7	18	29.7	42.2	54.9	67.2	78.3	86.6	90
	$\Delta\theta_i$	7.7	10.3	11.7	12.5	12.7	12.3	11.0	8.3	3.4

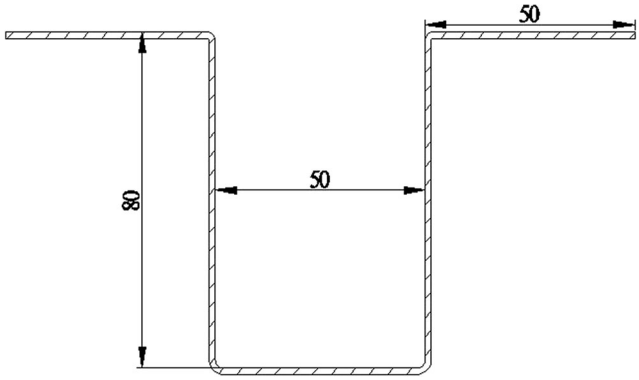

Fig. 3 Cross sectional shape and size of the hat-shaped steel

According to actual production experience and theoretical analysis, deformation of the sheet should be controlled at the beginning of forming to avoid edge tearing. In addition to this, Luo et al. [23] have found that the yield strength, and forming angle increment are sensitive to the springback and forming quality. Based on the research basis of a large number of scholars, the bite zone when the sheet enters the roll during the roll-forming process was fully considered. This is mainly due to the fact that the bite zone is the initial part of the forming sheet and it directly faces the straight roll shape during the forming process. The crimp of the bite zone is very obvious and the bending angle is too large to meet the forming dimension requirement. However, forming quality at the beginning of the sheet (the bite zone) is poor. There is a large amount of experimental data to prove that the probability of various product defects caused by excessive initial forming angle (excessive initial deformation) is greatly increased. Simultaneously, Kim et al. [24] selected the initial forming angles of 0°, 15°, and 30° to study the effect of the initial loading pattern on the longitudinal bowing during roll forming. The results show that the longitudinal bowing increases with the initial forming angle. Paralikas et al. [25] studied the longitudinal strain at the edge of the sheet at bending angles of 5°, 10°, 10°, and 15°, respectively. The study observed that the longitudinal strain at the edge was accumulated to reach the peak. Therefore, the forming angle of the first third pass in the roll forming process of this paper was set to not exceed 50% of the final forming angle, that is, $\theta_{N/3} \leq$ 50 % $\times\theta_N$, and

Table 3 Average mechanical properties of Q235 steel

Material properties	Value
Young's modulus (GPa)	206
Ultimate strength (MPa)	450
Yield limit (MPa)	235
Poisson's ratio	0.28
sheet thickness (mm)	1.5,4.0

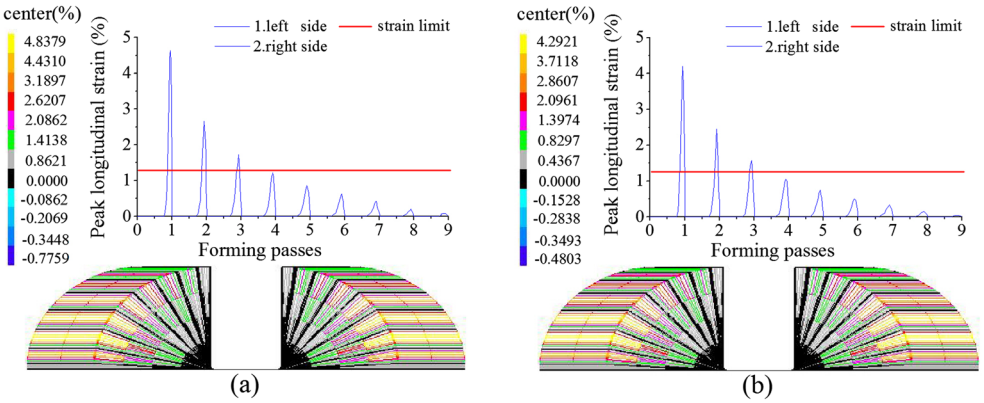

Fig. 4 Sheet thickness in roll-forming simulation based on four-boundary condition forming angle distribution function **a** 1.5 mm and **b** 4.0 mm

$$y_{N/3} = H\cos\theta_{N/3} \tag{4}$$

at this time. By combining this equation with the four-boundary condition in Eq. (2), a forming angle distribution function based on the five-boundary condition was constructed.

Assume that the projection track of the edge of the profile section in the horizontal plane, which follows a cubic curve, is a part of the quartic curve, and the expression of the quadratic curve is

$$y = Ax^4 + Bx^3 + Cx^2 + Dx + E. \tag{5}$$

When $x = N/3$, $y = H\cos\theta_{N/3}$; therefore, the five-boundary condition of Eq. (5) can be written as follows:

$$\begin{cases} \dfrac{dy}{dx} = 0, (\mathrm{x} = 0) \\ \dfrac{dy}{dx} = 0, (x = N) \\ y = H\cos\theta_{N/3}, (x = N/3) \\ y = H, (\mathrm{x} = 0) \\ y = H\cos\theta_0, (\mathrm{x} = N) \end{cases} \tag{6}$$

when $x = i$, $y_i = H\cos\theta_i$; thus, the forming angle in the ith pass θ_i in roll forming is

$$\cos\theta_i = 1 + \frac{81\cos\theta_{N/3} - 60}{4N^4} i^4 + \frac{-81\cos\theta_{N/3} + 64}{2N^3} i^3 + \frac{81\cos\theta_{N/3} - 72}{4N^2} i^2. \tag{7}$$

According to a previous study, the optimal interval of the first third-forming angle is $30\,\% \times \theta_0 \le \theta_{N/3} \le 35\,\% \times \theta_0$, and the distribution of forming angles when $\theta_{N/3} = 33\,\% \times \theta_0$ is selected. Then, $i = 1\ 2, \ldots, 9$ is substituted in Eq. (7) to obtain the forming angle distribution of the corresponding pass, as summarised in Table 2. In the present study, θ_0 is 90°, $\Delta\theta_i$ is the increment of the forming angle, $\theta_{N/3}$ is forming angle in the first third of the forming pass.

2.2 Effect of sheet thickness on roll forming based on four-boundary condition forming angle distribution function

In the present study, roll forming with multiple passes is simulated using DataM Copra RF v2005 SR1 software. The important simulation parameters are as follows: (1) DIN6935 method for calculation of sheet width; (2) Hauschild method for simulation; (3) 9 passes; (4) distance between two passes = 500 mm; and (5) surface meshing. A hat-shaped steel channel was selected as the research object, the cross-sectional shape and size of which are shown in Fig. 3. The mechanical properties of Q235 steel are summarised in Table 3.

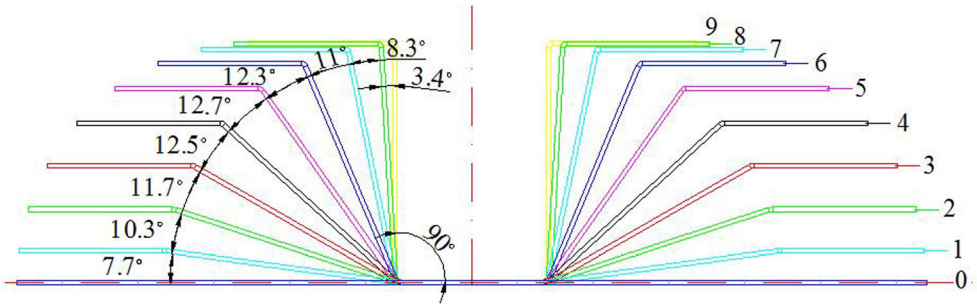

Fig. 5 Flower pattern of roll-forming progress

Roll-forming simulations of Q235 steel sheets with thicknesses of 1.5 mm and 4.0 mm based on the four-boundary condition forming angle distribution function are shown in Fig. 4, where the horizontal axis denotes the forming pass number, and the vertical axis denotes the peak longitudinal strain between two passes, that is, the normal strain, reflecting the deformation along the length direction of the sheet metal. The peak longitudinal strain on the left and right sides of the hat-shaped steel are represented by the superscripts (1) left side and (2) right side in the

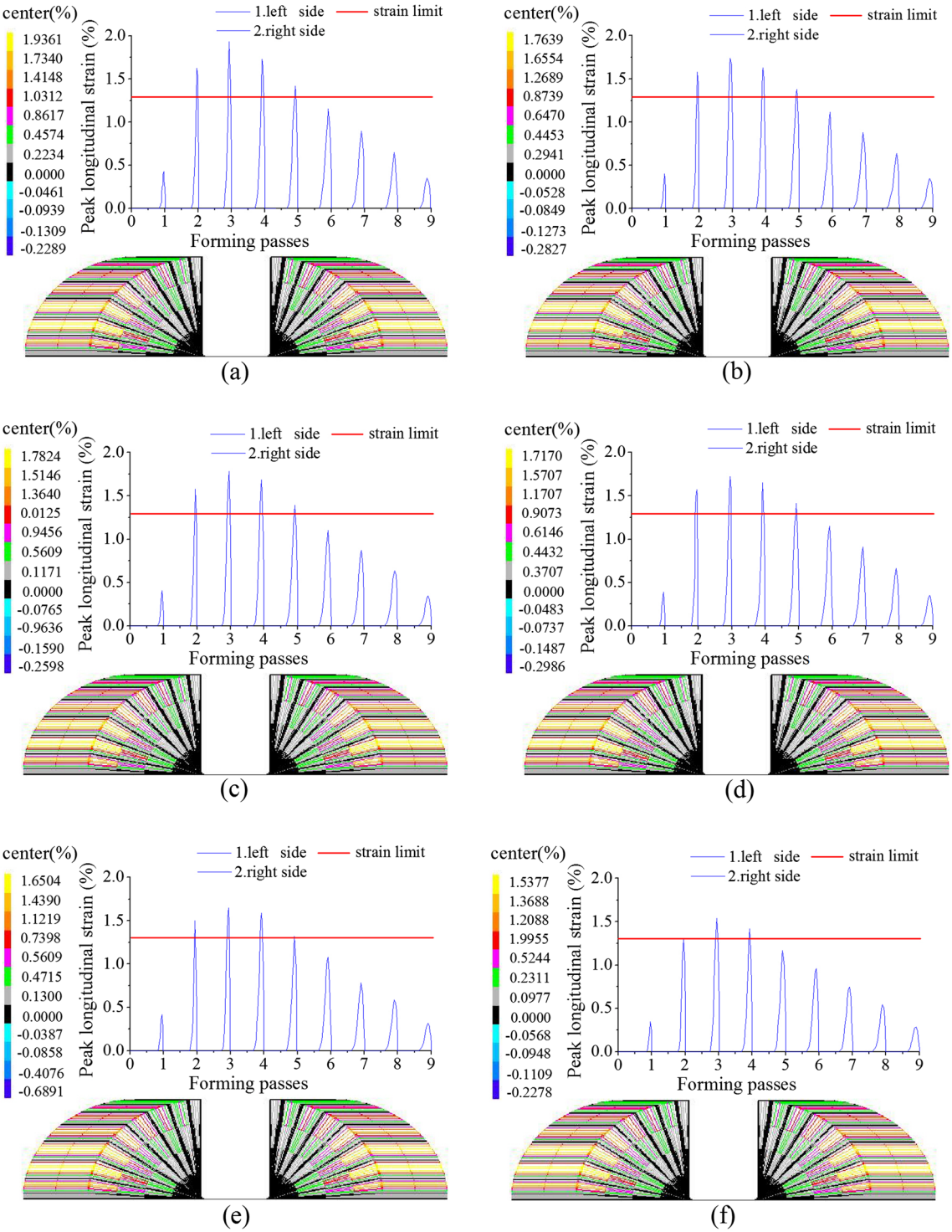

Fig. 6 Sheet thickness roll-forming simulation based on five-boundary condition forming angle distribution function **a** 0.5 mm, **b** 1.0 mm, **c** 1.5 mm, **d** 2.0 mm, **e** 4.0 mm, and **f** 6.0 mm

simulation diagram. Given that the hat-shaped steel is symmetrical, lines 1 and 2 coincide. Center % takes the sheet intermediate layer as the research object to study the peak longitudinal strain in roll forming process. The upper strain limit lines are depicted by horizontal lines on the graphs. The strain limit can be used as a reference to predict the plastic strain in longitudinal direction. In roll forming, the peak longitudinal strain in the first pass was 4.6% when the sheet thickness was 1.5 mm, peak longitudinal strain in the first pass was 4.1% when the sheet thickness was 4.0 mm, and peak longitudinal strain between two adjacent passes, shown in Fig. 4a, was higher than within a pass, shown in Fig. 4b. The peak longitudinal strain in the first third of Fig. 4 exceeds the strain limit, and it is evident from Table 1 that the peak longitudinal strain increases as the forming angle increases.

2.3 Effect of sheet thickness on roll forming based on five-boundary condition forming angle distribution function

When $\theta_{N/3} = 33\ \% \times \theta_0$, the flower pattern of roll forming progress based on the five-boundary condition forming angle distribution function is of the shape shown in Fig. 5.

Figure 6 demonstrates the roll forming simulation of Q235 steel with sheet thicknesses of 0.5 mm, 1.0 mm, 1.5 mm, 2.0 mm, 4.0 mm, and 6.0 mm based on the five-boundary condition forming angle distribution function. The six-thickness sheet strain curve shows that as the sheet enters the roll, the strain curve of each pass increases until the longitudinal strain peaks. Then, when the sheet breaks off the roll, the strain decreases abruptly and the peak longitudinal strain always occurs when just rolling. The peak longitudinal strain appeared in the third pass, and the peak longitudinal strain from the first pass to the third pass increased with increasing forming angle increments, and the peak longitudinal strain from the third pass to the ninth pass decreased gradually, but there was no obvious regularity between the peak longitudinal strain and the forming angle increment. Simultaneously, the difficulty and complexity of the reasonable distribution of forming angles in roll forming are explained. According to the simulation, the strain limit of Q235 steel was 1.3%, and the strain limit of Q235 steel did not change with increasing sheet thickness, which indicates that the strain limit was closely related to the properties of the material itself. In addition, the number of passes beyond the strain limit decreased as the sheet thickness increased. The peak longitudinal strain between passes in the simulation was recorded, and the strain curve plotted using this data is shown in Fig. 7. The six strain curves in Fig. 7 show that the peak longitudinal strain between passes decreases as sheet thickness increases.

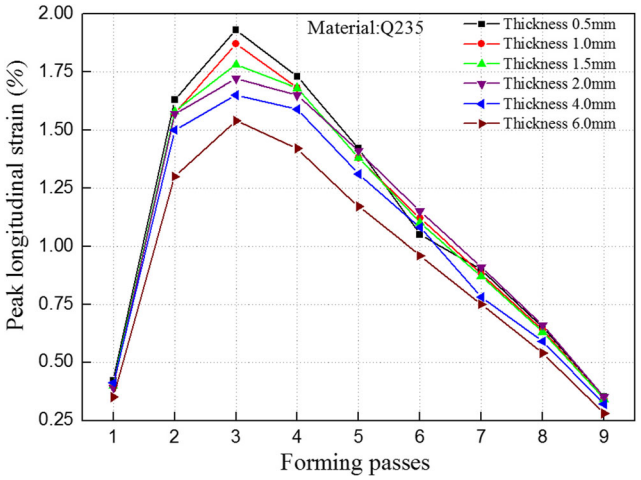

Fig. 7 Effect of sheet thickness on peak longitudinal strain between passes

2.4 Effect of material properties on roll forming based on five-boundary condition forming angle distribution function

Table 4 lists the basic material properties of SUS304 steel and DP780 steel. The roll-forming simulations of SUS304 steel and DP780 steel based on the five-boundary condition forming angle distribution function are shown in Fig. 8. The trend of the strain curves in this figure is similar, and the peak longitudinal strain appears in the third pass. The peak longitudinal strain from the first pass to the third pass increased with increasing forming angle increment. From the third pass to the ninth pass, the peak longitudinal strain decreased gradually, but the strain limit of the materials was 0.3 and 0.6, respectively. Between the two materials, the strain limit of Q235 steel was higher, and this difference in the strain limits of the materials shows that the strain limit of the material itself differs during roll forming. The peak longitudinal strain between passes in the simulation was recorded, and the strain curve is shown in Fig. 9. The strain curve in Fig. 9 shows that the peak longitudinal strain between passes increases with increasing of yield limit, and in the third pass, SUS304 steel has the lowest peak longitudinal strain.

Table 4 Mechanical properties of materials

Material properties	Material type	
	SUS304	DP780
Young's modulus (GPa)	193	218
Ultimate strength (MPa)	550	886
Yield limit (MPa)	228	578
Poisson's ratio	0.3	0.3
Sheet thickness (mm)	1.5	1.5

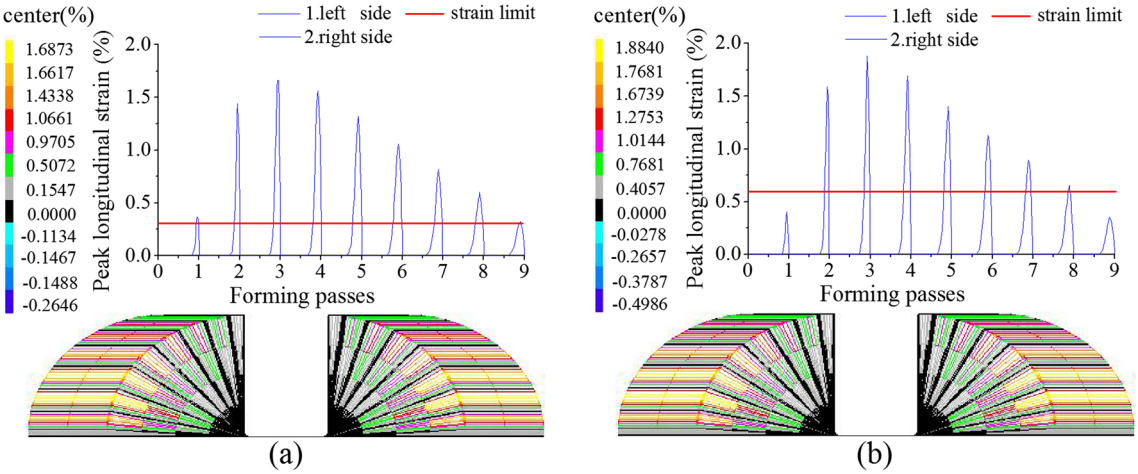

Fig. 8 Roll-forming simulation based on five-boundary condition forming angle distribution function considering of material properties of **a** SUS304 and **b** DP780

3 Experimental

The rolls were designed according to the results of the forming angle distribution shown in Table 2. The main parameters of the roll-forming machine used in the experiment are listed in Table 5. The roll-forming machine and the experimental products are shown in Figs. 10 and 11, respectively. The mechanical properties were measured by via tensile tests, according to ASTM-E8, using a universal material testing machine. The true stress-strain curves of the material is shown in Fig. 12. The sheet metal was not subjected to any special treatment before roll forming, and roll forming was performed at room temperature.

3.1 Microstructure based on five-boundary condition forming angle distribution function

The transverse strain in the sheet-bending zone was studied based on the microstructure of the sheet material, and the effect of roll forming on the microstructure of sheet was determined. The bending zone of the sheet is shown in Fig. 13, where panels (a), (b), and (c) show the outer, middle, and inner layers of the bend, respectively. The microstructure of the bending zone of all sheets was observed under 500× magnification by using a Nikon Industrial Microscope. The original microstructure of Q235 steel before roll forming in Fig. 14a shows square grains, and their length along the transverse and the thickness directions was 1–5 μm. Figure 14b shows the original microstructure of DP780 steel before roll forming, the grains of which are flat, and the grain lengths along the transverse and the thickness directions are 1–5 μm and 1–3 μm, respectively. As shown in Figs. 15a, 16a, 17a and 18a, in the outer layer of the bending zone of hat-shaped Q235 steel, all grains in the outer layer of the bending zone are significantly tensile along the transverse direction, and the grain length is concentrated at 3–6 μm. As shown in Figs. 15b, 16b, 17b and 18b, in the middle layer of the bending zone of hat-shaped Q235 steel, the shapes of all grains in the middle layer of the bending zone are virtually the same as those of the original grains shown in Fig. 14a. As shown in Figs. 15c, 16c, 17c and 18c, in the inner layer of the bending zone of hat-shaped Q235 steel, all grains in the inner layer of the bending zone are compressed along the thickness direction, and the grain thickness is concentrated at 1–3 μm.

Figures 15, 16, 17 and 18 indicate that the number of microscopic grains in the inner layer of the bending zone of Q235 steel is significantly higher than that in the outer layer

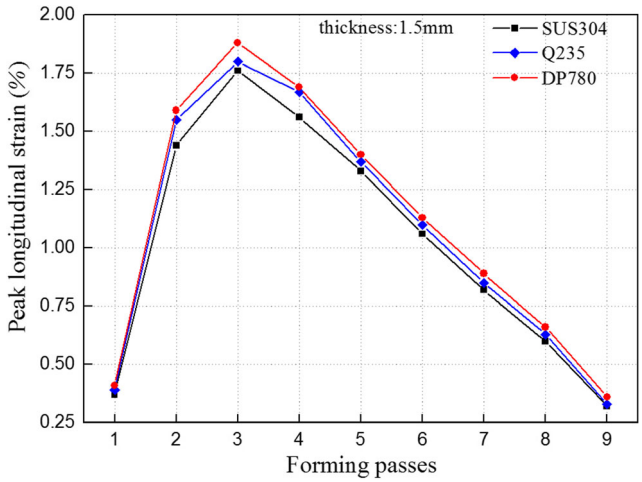

Fig. 9 Effect of material properties on peak longitudinal strain between passes

Table 5 Main parameters of roll forming machine in experiments

Forming parameters	Value
Forming speed (m/min)	5–10
Motor power (Kw)	7.5
Roller distances (mm)	500
Forming passes	9

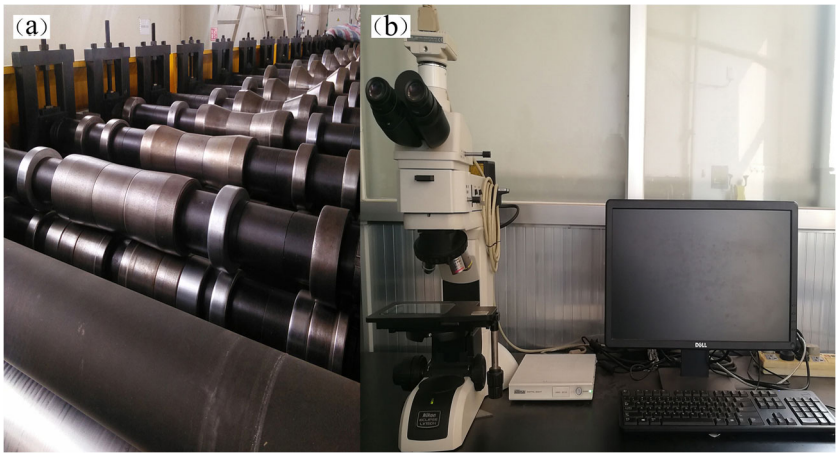

Fig. 10 Experimental equipment: **a** Cold roll forming machine and **b** Nikon Industrial Microscopes ECLIPSE LV150N

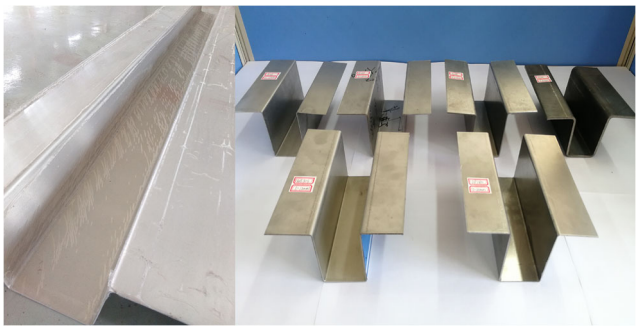

Fig. 11 Experimental products

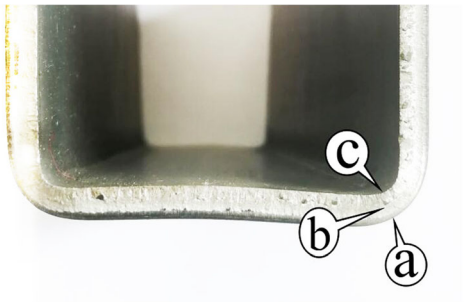

Fig. 13 Bending zone of hat-shaped steel

of the bending zone, and the change in grain size decreases with increasing sheet thickness. The number of grains in the same area increases due to the influence of compressive stress and strain in the inner layer of the bending zone. Similarly, the tensile stress and strain in the outer layer of the bending zone will result in a decrease in the number of grains in the same area. The stress and strain values of the bending zone of the sheet increase with increasing sheet thickness. Therefore, the microscopic grains in the inner layer of the bending zone are more and more severely compressed, and the microscopic grains in the outer layer of the bending zone are more and more severely stretched. Therefore, in the same area, there are more and more grains in the inner layer and fewer and fewer grains in the outer layer, but the changes of microscopic grains is gradually reduced. The microscopic grains in the

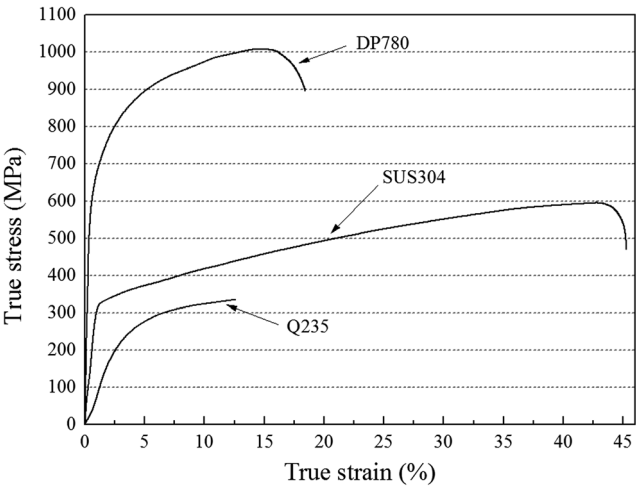

Fig. 12 True stress-strain curves of the materials of Q235, SUS304 and DP780 in 1.5mm thicknesses

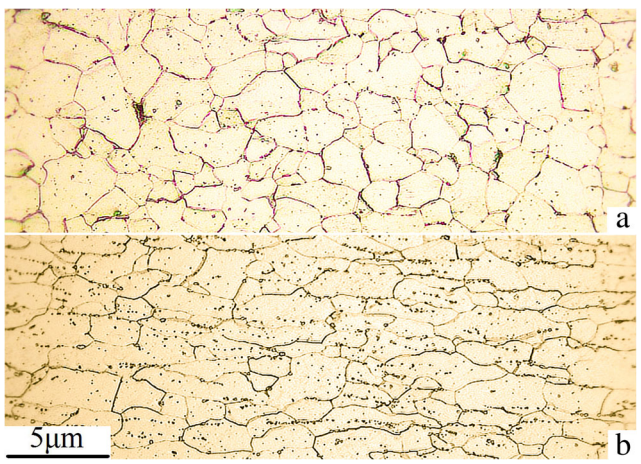

Fig. 14 Original microstructure of sheet before roll forming: **a** Q235 steel and **b** DP780 steel

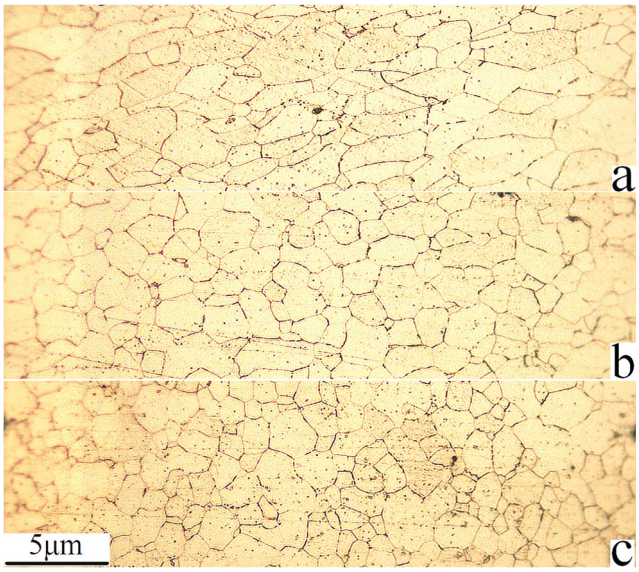

Fig. 15 Q235 steel microstructure for sheet thickness of 2.0 mm

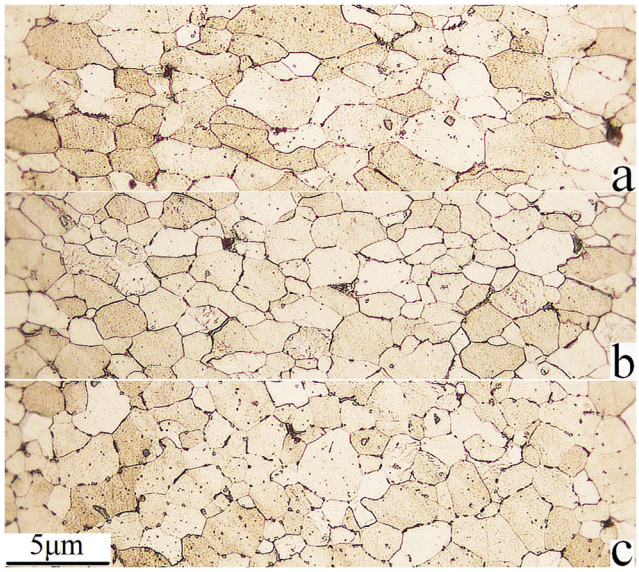

Fig. 17 Q235 steel microstructure for sheet thickness of 1.0 mm

bending zone of hat-shaped DP780 steel show the phenomenon of tension and compression in Fig. 19, but the change in grain size is not obvious. Simultaneously, the tensile strain of the grains in the outer layer of the bending zone along the sheet thickness direction is greater than the compressive strain in the inner layer, indicating that thickness reduction in the bending zone is inevitable. Q235 steel microscopic grains for thickness of 2.0 mm based on four-boundary condition is shown in Fig. 18. It can be seen from the figure that when the thickness of the sheet is the same, the grain size changes little compared with the microscopic grain size based on the distribution function of the five-boundary condition. However, the change of microscopic grains with sheet thickness is obvious. This indicates that the sheet thickness has a significant effect on the transverse strain of the forming zone.

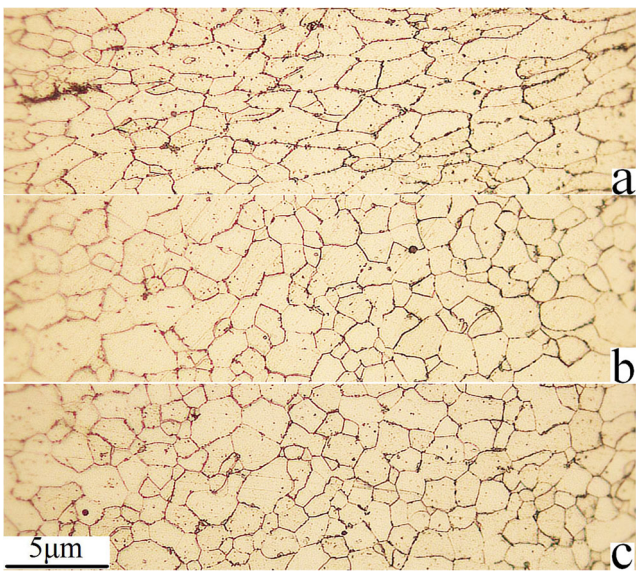

Fig. 16 Q235 steel microstructure for thickness of 1.5 mm

3.2 Longitudinal strain

According to the simulation results, in this experiment, we need to measure only the maximum line strain between passes. Given that the strain is the highest near the bending angle in the forming process, the experimental process can be relatively simplified, where only the strain near the bending angle must be measured. To facilitate data collection, we decided to measure only the values between the first to the fifth passes, including four groups of strain data along the forming direction between two passes. The strain values were measured using digital strain gauges connecting the strain rosette and the strain measuring points, as shown in Fig. 20. They

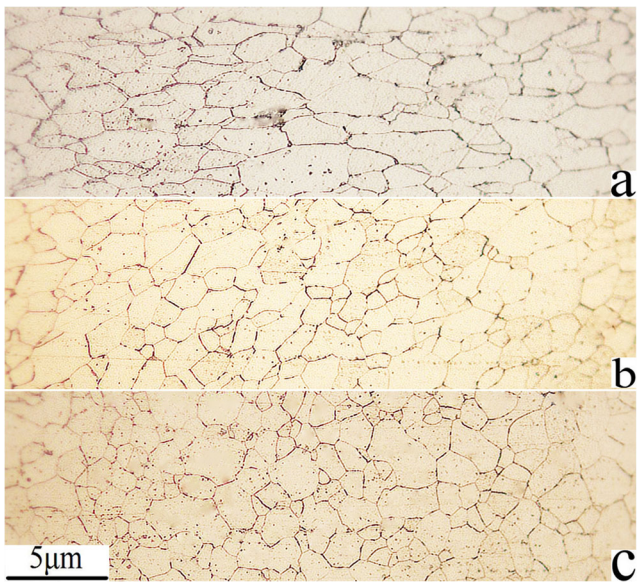

Fig. 18 Q235 steel microstructure for thickness of 2.0 mm based on four-boundary condition

Table 6 Strain recorded at each measuring point (unit με)

	Experiment material	Forming pass number			
		1–2	2–3	3–4	4–5
Peak longitudinal strain ($\mu\varepsilon$)	Q235 (1.5 mm)	15,755	18,208	15,945	13,770
	Q235 (2.0 mm)	15,665	17,505	15,608	14,080
	Q235 (4.0 mm)	16,903	18,552	16,500	13,786
	SUS304 (1.5 mm)	13,688	17,850	15,642	13,305
	DP780 (1.5 mm)	15,995	19,573	16,826	14,200

were numbered 1–3 from top to bottom, and the strain data were read directly from the digital strain gauge. The strain values recorded at each measuring point are presented in Table 6. The strains of Q235 steel with thicknesses of 1.5 mm, 2.0 mm and 4 mm, SUS304 steel with thickness of 1.5 mm, and DP780 steel with thickness of 1.5 mm are listed, and the strain values are the averages of the values recorded by the three strain gauges. The micro strain indicates the relative change in length: the unit symbol is "με".

According to Table 6, the effect of sheet thickness and material properties on the peak longitudinal strain between the first to the fifth passes is shown in Figs. 21 and 22, respectively. The peak longitudinal strain curve based on the five-boundary condition forming angle distribution function shows the same trend. The peak longitudinal strain of the first to the third passes increases gradually, while the peak longitudinal strain of the third to the fifth passes decreases gradually. The peak longitudinal strain of the first third passes based on the four-boundary condition forming angle distribution function was significantly higher than the peak longitudinal strain based on the five-boundary condition forming angle distribution function, and the peak longitudinal strain decreased from 4.6% to less than 2%. For Q235 steel, in Fig. 21, when the thickness was 1.5 mm, the measured peak longitudinal strain was the maximum, and when the thickness was 4.0 mm, the measured peak longitudinal strain was the minimum; it was found that the peak longitudinal strain based on the five-boundary condition forming angle distribution function decreased as the sheet thickness increased. For the thickness of 1.5 mm in Fig. 22, the peak longitudinal strain of SUS304 steel was the lowest, but the difference between the peak longitudinal strains of SUS304 steel and Q235 steel was small, and the peak longitudinal strain of DP780 steel was the highest. This indicates that the peak longitudinal strain is closely related to material properties. Simultaneously, the simulation data and the experiment measurements were compared to verify the reliability of the simulation and the rationality of the five-boundary condition forming angle distribution function. The peak longitudinal strain of the forming angle based on the four-boundary condition distribution is very high in the first and second passes, as shown in Fig. 23. The peak longitudinal strain of the third to ninth passes based on the five-boundary condition is slightly higher than the peak longitudinal strain based on the four-boundary condition. The peak longitudinal strain occurs in the opposite direction when the roll bite sheet and the sheet are separated from the roll, as shown in A-A in Fig. 23, but the strain is very small, which

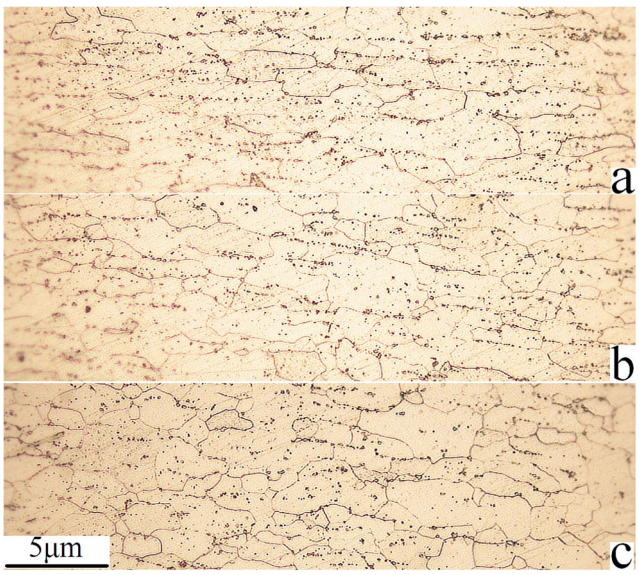

Fig. 19 DP780 steel microstructure for sheet thickness of 1.5 mm

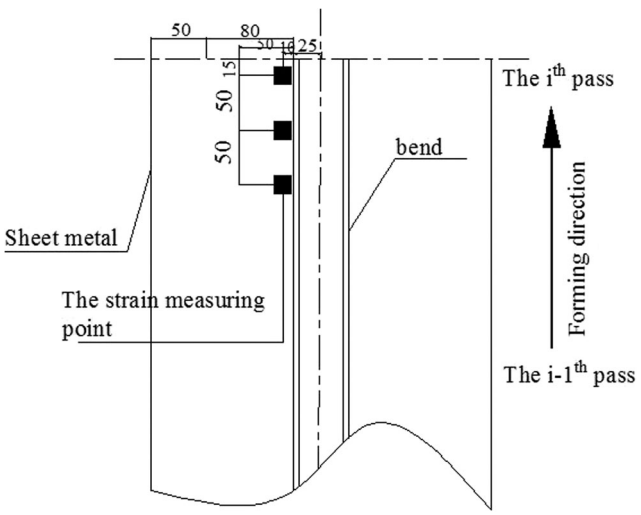

Fig. 20 Strain measurement points

Table 7 Experimental measurement data of forming angle

Experimental group	Forming pass number									
	0–1	1–2	2–3	3–4	4–5	5–6	6–7	7–8	8–9	0–9
Q235 (1.0 mm)	7.6	17.4	29.1	41.7	54.5	66.9	78.1	86.4	89.9	88.3
Q235 (1.2mm)	7.6	17.5	29.2	41.7	54.6	67.0	78.2	86.5	89.9	88.8
Q235 (1.5 mm)	7.7	17.6	29.4	42.0	54.7	67.1	78.3	86.6	90.0	88.8
Q235 (2.0 mm)	7.7	17.8	29.5	42.1	54.8	67.1	78.3	86.6	90.0	89.2
Q235 (4.0mm)	7.7	17.9	29.5	42.1	54.8	67.2	78.3	86.6	90.0	89.5
SUS304 (1.5 mm)	7.7	17.6	29.4	42.0	54.7	67.0	78.2	86.5	89.9	89.0
DP780 (1.5 mm)	7.6	17.4	29.0	41.6	54.4	66.7	77.9	86.3	89.9	87.9
Four-boundary(1.5 mm)	13.8	28.2	41.5	53.8	65.2	74.9	82.6	87.9	90.0	87.7

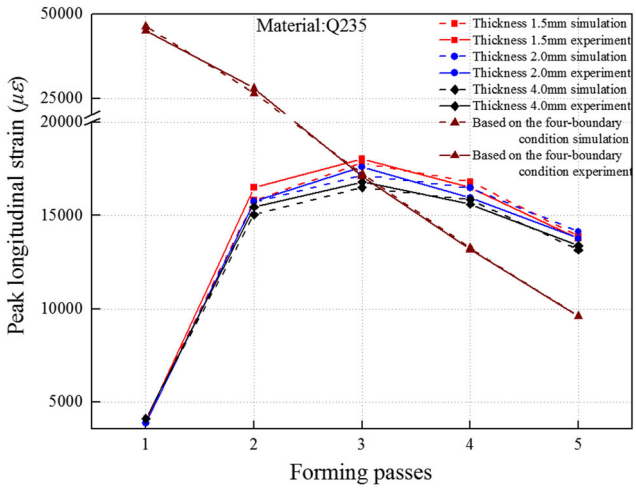

Fig. 21 Strain as a function of sheet thickness

is an elastic strain and will recover after forming. In the manuscript, scholars' studies on peak longitudinal strain are listed, and they all agree that high peak longitudinal strain is an important cause of product defects, especially in the first pass,

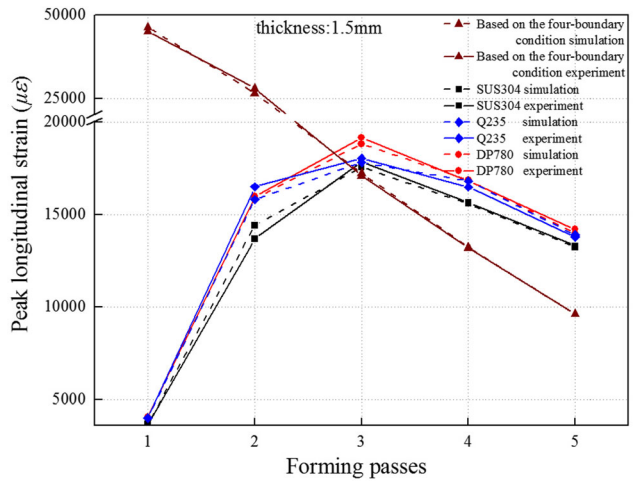

Fig. 22 Strain as a function of material

excessive peak longitudinal strain will directly affect the bite of sheet and roll. Hui and Wang. [26] have reached the same conclusion.

3.3 Springback

The forming angle for each pass of the experimental product based on the five-boundary condition forming angle distribution function was measured in Fig. 24 and recorded in Table 7, but each group angle is the average of two experimental products. The difference between the forming angle during the simulation and the forming angle during the experimental measurement is called springback, and the definition of springback is shown in Fig. 25.

According to Table 7, the springback angle between adjacent passes and that of the first to ninth passes of successive forming was calculated. The springback angle of the first third pass of the forming angle distribution function based on the four-boundary condition was significantly higher than that of the five-boundary condition forming angle distribution function. The springback angle of first pass

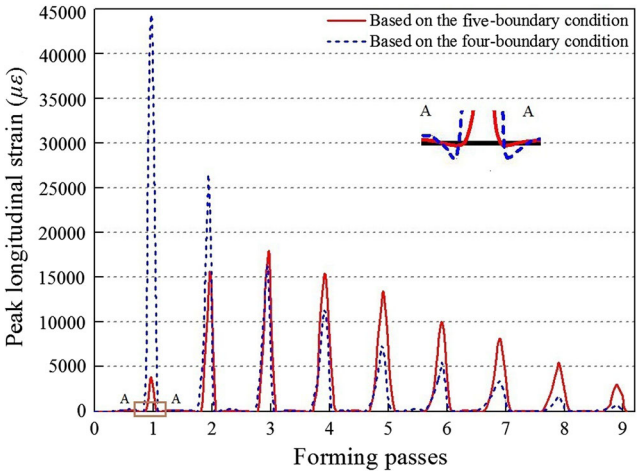

Fig. 23 Measurement of peak longitudinal strain based on four- and five-boundary condition

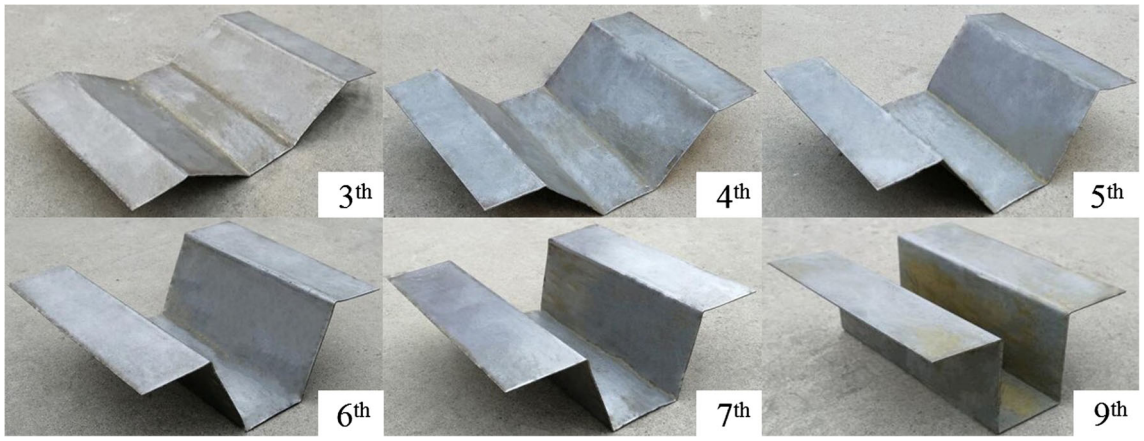

Fig. 24 Third to seventh and ninth experimental products

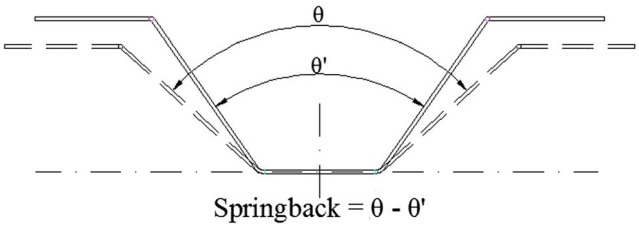

Fig. 25 Definition of Springback

was 1.2° and that of the first to ninth passes of continuous forming was 2.3°, as determined based on the four-boundary condition forming angle distribution function. However, the springback angle between passes determined based on the five-boundary condition was less than 0.7°. As shown in Fig. 26, the springback decreases with the increase of sheet thickness under the condition of a certain roll radius. There is a linear relationship between springback and thickness of sheet. The change of sheet thickness will directly affect the springback after unloading. The main reason for the analysis is that under the same bending radius, the surface strain and stress value of the sheet with large thickness is larger, and there are more plastic deformation materials, so the springback will be reduced. For the sheet thickness of 1.5 mm, as in Fig. 27, the springback angle of DP780 steel was significantly higher than that of SUS304 steel and Q235 steel. The springback angles of SUS304 steel and Q235 steel were essentially equal, indicating that material properties significantly influenced the springback angle of the sheet. Simultaneously, it was verified that the five-boundary condition forming angle distribution function could effectively reduce the springback angle of the sheet.

4 Conclusions

In this study, hat-shaped steel samples were used as the research object to verify that the peak longitudinal strain increases with increasing forming angle. It was further verified that the peak longitudinal strain of the first third pass when $\theta_{N/3} = 33\ \% \times \theta_0$ based on the five-boundary condition forming

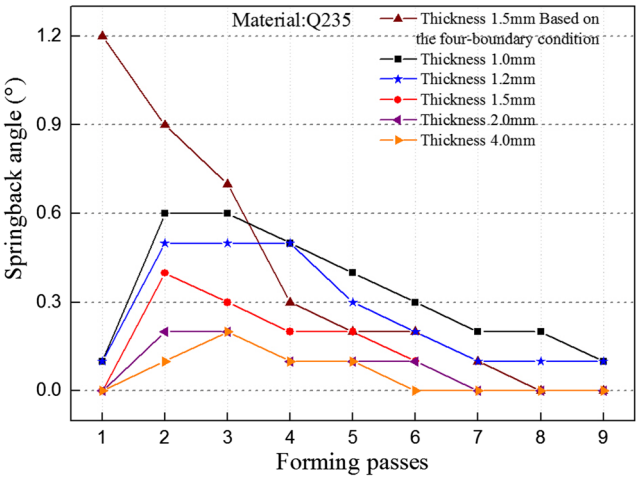

Fig. 26 Springback angle as a function of sheet thickness

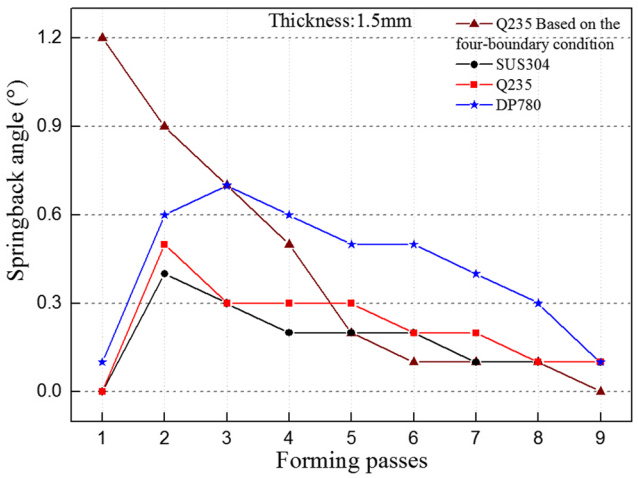

Fig. 27 Springback angle as a function of material

angle distribution function was significantly lower than that based on the four-boundary condition. The peak longitudinal strain decreased from 4.64 to 1.78%.

The effects of material properties and sheet thickness on the roll forming process were studied based on the five-boundary condition forming angle distribution function. The peak longitudinal strain decreases with the sheet thickness increase, while the transverse strain in the sheet-bending zone during roll forming increases with the sheet thickness increase. The springback decreases with the increase of sheet thickness under the condition of a certain roll radius. There is a linear relationship between springback and thickness of sheet. The change of sheet thickness will directly affect the springback after unloading. The first to ninth pass continuous forming springback angle was only 0.5° in the paper.

A comparison of the properties of SUS304 steel, Q235 steel and DP780 steel showed that the peak longitudinal strain increased with increasing yield limit. The springback angle of DP780 steel was significantly higher than that of SUS304 steel and Q235 steel, and the springback angle of the sheet was closely related to the yield limit of the material.

Funding information The authors would like to acknowledge the financial support provided by Shandong Provincial Natural Science Foundation, China (ZR2018MEE022), the National Natural Science Foundation of China (grant no.51705295), Taishan Scholarship Project of Shandong Province, China (no. tshw20130956), and Scientific Research Foundation of Shandong University of Science and Technology for Recruited Talents (2017RCJJ027).

Publisher's note Springer Nature remains neutral with regard to jurisdictional claims in published maps and institutional affiliations.

References

1. Salem J, Champliaud H, Feng Z, Dao TM (2016) Experimental analysis of an asymmetrical three-roll bending process. Int J Adv Manuf Technol 83(9–12):1823–1833
2. Cai ZY, Guan DB, Wang M, Li MZ (2014) A novel continuous roll forming process of sheet metal based on bended rolls. Int J Adv Manuf Technol 73(9–12):1807–1814
3. Asl YD, Sheikhi M, Anaraki AP, VP R, Gollo MH (2016) Fracture analysis on flexible roll forming process of anisotropic Al6061 using ductile fracture criteria and FLD. Int J Adv Manuf Technol 91(5–8):1–12
4. Zhuang W, Hua L, Wang X, Liu YX, Han XH, Dong LY (2015) Numerical and experimental investigation of roll-forging of automotive front axle beam. Int J Adv Manuf Technol 79(9–12):1761–1777
5. Jiao J, Rolfe B, Mendiguren J, Weiss M (2016) An analytical model for web-warping in variable width flexible roll forming. Int J Adv Manuf Technol 86(5–8):1541–1555
6. Bidabadi BS, Naeini HM, Tehrani MS, Barghikar H (2016) Experimental and numerical study of bowing defects in cold roll-formed, U-channel sections. J Constr Steel Res 118:243–253
7. Bidabadi BS, Naeini HM, Tafti RA, Barghikar H (2016) Experimental study of bowing defects in pre-notched channel section products in the cold roll forming process. Int J Adv Manuf Technol 87(1–4):997–1011
8. Liu CF, Zhou WL, Fu XS, Chen GQ (2015) A new mathematical model for determining the longitudinal strain in cold roll forming process. Int J Adv Manuf Technol 79(5–8):1055–1061
9. Lindgren M (2007) Cold roll forming of a U-channel made of high strength steel. J Mater Process Technol 186(1–3):77–81
10. Yan Y, Wang H, Li Q, Qian B, Mpofu K (2014) Simulation and experimental verification of flexible roll forming of steel sheets. Int J Adv Manuf Technol 72(1–4):209–220
11. Liu XL, Cao JG, Chai XT, He ZL, Liu J, Zhao RJ (2017) Experimental and numerical prediction of the local thickness reduction defect of complex cross-sectional steel in cold roll forming. Int J Adv Manuf Technol 6:1–12
12. Kim JH, Woo YY, Hwang TW, Han SW, Moon YH (2016) Effect of loading pattern on longitudinal bowing in flexible roll forming. J Mech Sci Technol 30(12):5633–5639
13. Abeyrathna B, Rolfe B, Hodgson P, Weiss M (2016) An extension of the flower pattern diagram for roll forming. Int J Adv Manuf Technol 83(9–12):1683–1695
14. Abeyrathna B, Rolfe B, Hodgson P, Weiss M (2016) A first step towards a simple in-line shape compensation routine for the roll forming of high strength steel. Int J Mater Form 9(3):423–434
15. Han ZW, Liu C, Lu WP, Ren LQ, Tong J (2005) Spline finite strip analysis of forming parameters in roll forming a channel section. J Mater Process Technol 159(3):383–388
16. Paralikas J, Salonitis K, Chryssolouris G (2009) Investigation of the effects of main roll-forming process parameters on quality for a V-section profile from AHSS. Int J Adv Manuf Technol 44(3–4):223–237
17. Zeng G, Li SH, Yu ZQ, Lai XM (2009) Optimization design of roll profiles for cold roll forming based on response surface method. Mater Des 30(6):1930–1938
18. Abeyrathna B, Rolfe B, Hodgson P (2017) Local deformation in roll forming. Int J Adv Manuf Technol 88(9–12):1–11
19. Rezaei R, Naeini HM, Tafti RA, Kasaei MM, Mohammadi M, Abbaszadeh B (2017) Effect of bend curve on web warping in flexible roll formed profiles. Int J Adv Manuf Technol 93(9–12):1–12
20. Liu W, Huang K (2016) Research on the three-roll-push-bending forming rules for improving processing precision. Int J Adv Manuf Technol 90(1-4):763–773
21. Ona H, Jimma T, Kozono H, Nakako T (2008) Computer-aided design for cold roll forming of light-gauge steel members. Trans Jpn Soc Mech Eng 55(512):1116–1121
22. Halmos GT (2006) Roll forming handbook. Crc Press
23. Luo XL, Yu ZQ, Li SH, Zeng G (2008) Finite element analysis of the springback in high strength steel roll forming. Journal of Plasticity Engineering 42(5):744–747
24. Kim JH, Woo YY, Hwang TW, Han SW, Moon YH (2016) Effect of loading pattern on longitudinal bowing in flexible roll forming. Journal of Mechanical Science & Technology 30(12):5633–5639
25. Paralikas J, Salonitis K, Chryssolouris G (2009) Investigation of the effects of main roll-forming process parameters on quality for a V-section profile from AHSS. Int J Adv Manuf Technol 44(3-4):223–237
26. Hui XJ, Wang XM (2018) Forming quality analysis on the cold roll forming C-channel steel. Mater 11:1911–1922